Physics of Fluids

Pulsatile twin parallel jets through a flexible orifice with application to edge-to-edge mitral valve repair

Cite as: Phys. Fluids **32**, 121702 (2020); https://doi.org/10.1063/5.0025859
Submitted: 19 August 2020 • Accepted: 04 November 2020 • Published Online: 02 December 2020

Maziar Sargordi, Anna Chtchetinina, Giuseppe Di Labbio, et al.

Pulsatile twin parallel jets through a flexible orifice with application to edge-to-edge mitral valve repair

Cite as: Phys. Fluids 32, 121702 (2020); doi: 10.1063/5.0025859
Submitted: 19 August 2020 • Accepted: 4 November 2020 •
Published Online: 2 December 2020

Maziar Sargordi,[a] Anna Chtchetinina, Giuseppe Di Labbio, Hoi Dick Ng, and Lyes Kadem

AFFILIATIONS

Department of Mechanical, Industrial and Aerospace Engineering, Concordia University, Montreal, Quebec H3G 1M8, Canada

[a]Author to whom correspondence should be addressed: lcfd@encs.concordia.ca

ABSTRACT

Edge-to-edge repair is a procedure introduced to overcome mitral valve regurgitation. However, it leads to an unusual flow in the left ventricle characterized by twin parallel pulsed jets. This type of flow has not been extensively investigated in the literature. We set up a basic experiment to better characterize this type of flow from a fundamental point of view. Planar time-resolved particle image velocimetry measurements were performed downstream of three configurations of mitral valves corresponding to healthy and repaired valves. The flow field is characterized using velocity profiles, viscous energy dissipation, and time-frequency spectra, and their potential clinical impact is highlighted.

The mitral valve (MV) is located between the left atrium and the left ventricle (LV) and plays an essential role in the optimal filling of the left ventricle. Several conditions, including rheumatic fever, endocarditis, and cardiomyopathy, may affect the MV and lead to an abnormal backflow from the LV to the left atrium called mitral regurgitation (MR). Around 10% of people over the age of 75 suffer from MR and it is the second most common disease requiring surgery in Europe.[1–3] Surgical mitral valve intervention is currently considered the best option for the treatment of symptomatic patients with severe degenerative MR.[1,4] Several reports have indicated the superiority of MV repair over replacement based on it having a better preservation of LV function, lower thrombus formation, and higher survival rates.[5] The current MV repair procedures include annuloplasty, quadrangular resection, resuspension of leaflets, and edge-to-edge repair (ETER). Edge-to-edge repair (ETER) was pioneered by Alfieri *et al.*[6] This open-heart surgery technique consists of suturing the free edges of the MV leaflets at the location where there is regurgitation. Almost half of the patients with symptomatic severe MR are, however, considered at high risk and not eligible to undergo an open-heart surgery.[7] For those patients, ETER is still an option, thanks to a minimally invasive approach using MitraClip or the newly developed PASCAL[8] transcatheter devices. ETER significantly modifies the flow patterns in the LV and leads to an unusual double-orifice (DO) configuration during MV opening. Under such a valve opening configuration, the induced flow in the LV is mostly unknown. Numerical simulations done by Maisano *et al.* revealed that velocity profiles downstream of a DO MV are close to the one obtained downstream of a healthy single orifice (SO) MV.[9] In another numerical study by Hu *et al.*,[10] it was demonstrated that a DO MV induces significant energy losses. They also showed that ETER significantly lowers the LV filling efficiency.

From a fluid dynamics point of view, ETER leads to a very interesting and rich flow physics configuration consisting of pulsatile twin parallel jets. Studies on twin jets are gaining a lot of interest but are limited in the literature to steady round jets with[11–16] or without crossflow.[17–19] In a recent interesting study, Zang and New performed particle image velocimetry (PIV) measurements to investigate the effect of nozzle spacing on vortical structures in twin round jets.[18] When the distance between the nozzle centers was 1.5 to 2 diameters, they observed that vortices of alternating sign in the inner shear layers were staggered, acting like the wake vortices behind a bluff body. However, for nozzle spacing higher than three diameters, jets behaved like two separate single jets due to the limited interaction between the induced vortices. Regarding studies on pulsatile jets, they are limited to single orifice

configurations, with the exception of Athanassiadis and Hart.[20] In their study, they evaluated the induced thrust generated by twin vortex ring formation with applications to underwater robots. They showed that the interaction between the two vortex rings, due to a small spacing between the orifices, leads to a significant reduction in the induced thrust. Regarding ETER, Jeyhani *et al.* conducted an *in vitro* study to evaluate the hemodynamic changes following a simulated ETER.[21] They showed that ETER increases the number of regions with significantly high Reynolds and viscous shear stresses in the LV.

The above literature review illustrates that there is a knowledge gap regarding pulsatile twin jets. Since the flow in the LV is complex and highly three-dimensional, we believe it will be of interest to first experimentally investigate the flow induced by ETER from a fundamental perspective in the case of an unbounded flow while still relating our findings to the clinical setting. More specifically, two physiologically relevant characteristics are explored: the pumping function and the risk of blood cell damage. The pumping function is examined by computing the impact of ETER on viscous energy dissipation (VED), while the risk of blood cell damage is evaluated by performing a time-frequency analysis using wavelet transforms.

The experimental setup used in this study consists of a piston-cylinder device of small diameter submerged in a large transparent Plexiglas water tank of size $30.5 \times 94 \times 63$ cm^3 (see Fig. 1). The flow is driven by the piston using a pump control system (SuperPump, ViVitro Systems, Inc., Victoria, BC, Canada). The piston movement is controlled by a function generator through a custom user interface created with LabVIEW (National Instruments, Austin, TX, USA). The duration of the piston motion is 0.25 s. Normalized by the duration of the recording (T = 1 s), this represents a dimensional time of t/T = 0.25. A 32-mm circular nozzle with a healthy or a manually sutured elastic model of the mitral valve is attached to the end of the piston-cylinder where the flow emerges into the water tank. The model of the mitral valve, with a 32 mm inner diameter, was created by coating successive layers of latex (Environmental Technology, Inc., MI, USA; density: 0.94 at 24 °C). Three different conditions are investigated in this study: (1) a normal, un-sutured, healthy mitral valve configuration leading to a single orifice (SO) jet; (2) a mitral valve model with a suture in the middle, maintaining a symmetric geometry; and (3) a mitral valve model with an eccentric suture, creating an asymmetric geometry. The suture is created by locally sowing the two leaflets of the valve together. The suture is about 6 mm in length. A schematic of the valves is provided in Fig. 1. In this experiment, three formation times, L/D, are considered: 1.5, 1.9, and 2.5, representing the ratio of the length to the diameter of the ejected fluid column.[22] The choice of this range is based on flow conditions that may exist before edge-to-edge repair in patients with functional mitral regurgitation and dilated cardiomyopathy. Gharib *et al.* have shown that, in healthy patients, L/D typically ranges between 3.5 and 5.5, but in patients with dilated cardiomyopathy, L/D values dropped significantly to the range between 1.5 and 2.5.[23] Table I summarizes the experimental conditions in terms of configurations, formation times, and the resulting average Reynolds numbers.

Time-resolved particle image velocimetry. A LaVision (LaVision GmbH, Gottingen, Germany) PIV system is used for time-resolved planar acquisitions and post-processing of the velocity fields. The

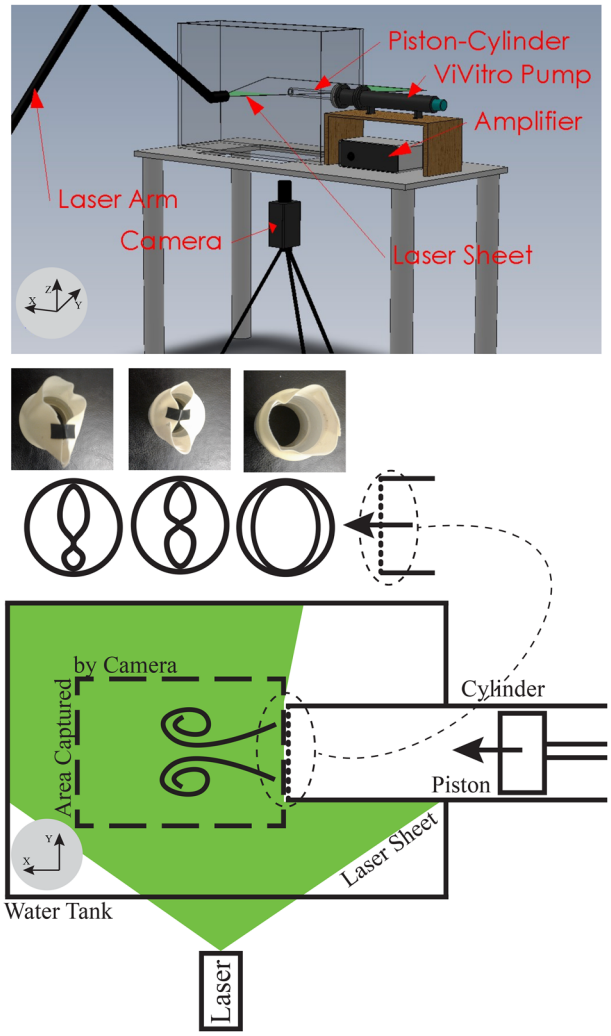

FIG. 1. Illustration and schematic of the experimental setup and the three orifice configurations used in this study. The dashed line delimits the region of interest captured by the camera.

averaged values reported are based on 350 instantaneous measurements. The uncertainty in the velocity is less than 5% when considering the major sources of errors, as described in the studies of Raffel *et al.*,[24] Adrian *et al.*,[25] and Sciacchitano.[26] More information

TABLE I. Average Reynolds number for different configurations.

	Single orifice	Symmetric double orifice	Asymmetric double orifice
L/D = 1.5	2733	9 842	7 105
L/D = 1.9	3751	11 224	10 143
L/D = 2.5	3842	12 887	10 692

regarding the PIV measurements can be found in the supplementary material.

Kinetic energy and viscous energy dissipation. The total flow kinetic energy is derived from the time-resolved velocity measurements using the following formulation:

$$KE = \frac{\rho}{2}\iint (u^2 + v^2)dxdy. \quad (1)$$

The rate of viscous energy dissipation (VED) represents the irreversible conversion of flow kinetic energy to internal energy.[27] It is a good indicator of energy loss in the flow field due to viscous stresses. Following the work done by Pedrizzetti and Domenichini,[28] Stugaard *et al.*,[29] and Di Labbio and Kadem,[30] VED for a 2D velocity field is calculated according to

$$VED = \mu \iiint \left(2\left(\frac{\partial u}{\partial x}\right)^2 + 2\left(\frac{\partial v}{\partial y}\right)^2 + \left(\frac{\partial u}{\partial y} + \frac{\partial v}{\partial x}\right)^2\right)dxdydt. \quad (2)$$

In Eqs. (1) and (2), u and v are the velocity components in the x and y directions, μ is the fluid dynamic viscosity, and ρ is the fluid density. The spatial derivatives in the VED formulation are calculated using a fourth-order compact-Richardson scheme (see the work of Etebari and Vlachos for details).[31] This scheme has been shown to limit noise amplification and is well adapted to PIV measurements. The integration of KE and VED was performed over all the field of view.

From a clinical point of view, VED is an important index that reflects the spatial dispersion of blood flow and indicates energy dissipation caused by viscosity. In the human heart, an increase in VED leads to an increase in the required pumping power of the LV. For better illustration, the reported values for KE and VED are filtered using empirical mode decomposition[32] where the first intrinsic mode functions, containing high frequencies, are removed.

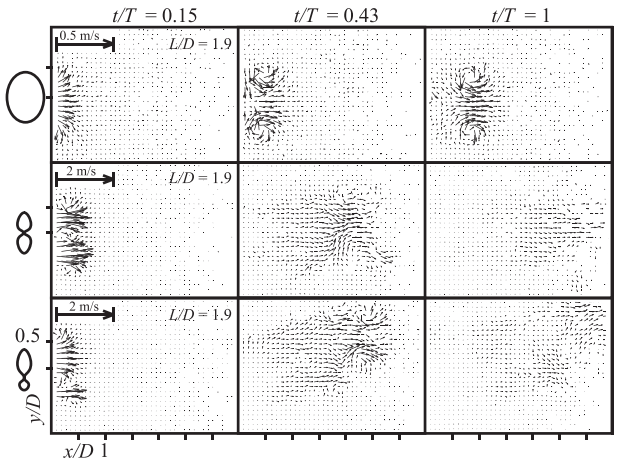

FIG. 2. Velocity field snapshots for all the configurations tested for an *L/D* value of 1.9 at three different time instants (*t/T* = 0.15, 0.43, and 1). For other *L/D* values, see the videos in the supplementary material. Multimedia views of POD-filtered velocity and vorticity fields: circular orifice, symmetric double orifice, and asymmetric double orifice. Multimedia views: https://doi.org/10.1063/5.0025859.1; https://doi.org/10.1063/5.0025859.2; https://doi.org/10.1063/5.0025859.3

Time-frequency spectra. In order to investigate the presence of turbulence in the flow downstream of the valve, the time-frequency spectra of recorded velocity signals at various selected points are generated using the continuous wavelet transform. For this purpose, the complex Morlet wavelet is used for all cases.

Validation of the single orifice configuration. The first step in this study was to validate the flow through the single orifice configuration against the results of Gharib *et al.*[22,33] The reader is referred to the supplementary material for a detailed validation for *L/D* values of 1.5, 1.9, and 2.5.

Single orifice vs double orifice configurations. Figure 2 (Multimedia view) displays the snapshots of the velocity and vorticity fields for the three configurations tested in this study (single orifice, symmetric double orifice, and asymmetric double orifice). Here, for clarity and conciseness, only the results for an *L/D* = 1.9 are displayed. Other *L/D* leads to similar flow configurations albeit different velocity and vorticity amplitudes. One can notice that the single orifice configuration leads to a vortex ring that is transported downstream without a trailing jet, while the double orifice configurations lead to more complex flow patterns. The jets in the double orifice configurations travel up to three times faster than in the single orifice jet and induce more shear in the flow field. Another interesting aspect is the side deflection of the upper, larger, jet mostly observed in the case of the asymmetric double orifice configuration (see also the videos

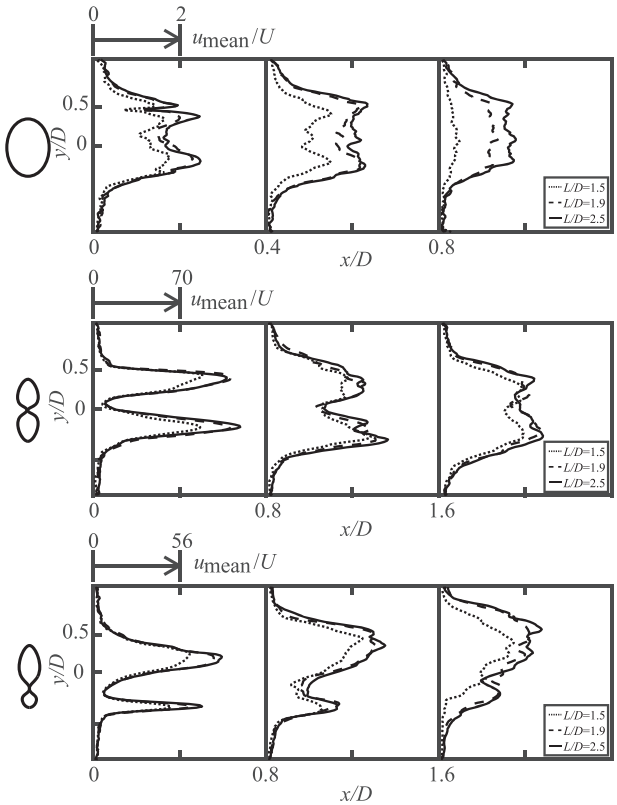

FIG. 3. Normalized time-averaged velocity profiles for all the orifice configurations at different *x/D* values.

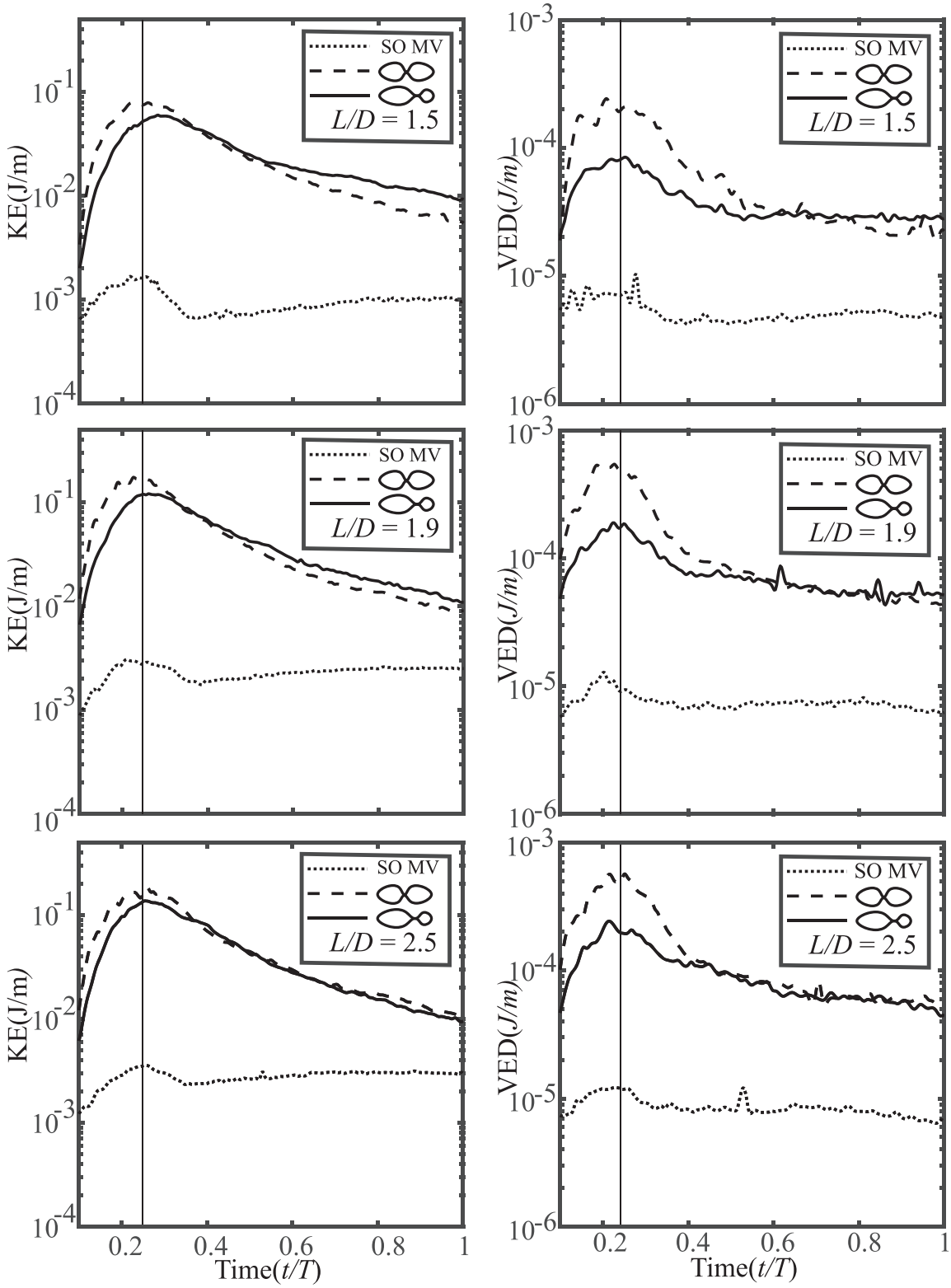

FIG. 4. Temporal evolution of the total in-plane kinetic energy (left) and total in-plane viscous energy dissipation (right).

in the supplementary material). Indeed, in the case of steady twin jets with small spacing, studies have shown that the inner shear layer exhibits complex fluid dynamics characterized by confined counter-rotating vortical structures and a mutual destabilizing effect of one jet on the other.[11,12,18] In the case of the asymmetric orifice, the flow through the larger orifice exhibits a vortex ring with its lower part, in the inner shear layer, interacting with the jet leaving the smaller orifice. When the piston stops, this interaction seems to lead to a deflection of the upper jet. Further studies including more cases are, however, required in order to better characterize the flow dynamics in such configuration and the resulting jet deflection.

Figure 3 displays the normalized time-average velocity profiles for $L/D = 1.9$. In order to compare with the single orifice configuration, the profiles for the double orifice configurations are normalized with respect to the mean jet exit velocity of the single orifice configuration. The single orifice configuration rapidly leads to a flat velocity profile just downstream of the orifice. This is consistent with what is expected downstream of a native healthy mitral valve. However, the double orifice configuration resulting from ETER leads to a double jet velocity profile with elevated localized velocity gradients.

Kinetic energy and viscous energy dissipation. The left panels of Fig. 4 display the time evolution of the KE. The results show that the single orifice configuration results in a lower in-plane flow kinetic energy, and that after the driving piston stops at $t/T = 0.25$, the vertical line in Fig. 4, this kinetic energy is quite well conserved. This is consistent with the concept of optimal transport of energy with a vortex ring at low formation times.[23] A progressive increase is also noticeable after the piston has stopped and can be attributed to a partial closure of the valve leaflets and a decrease in the vortex ring size (see the videos in the supplementary material). However, this has still to be confirmed in future studies. High in-plane kinetic energy values are generated during the movement of the piston followed by a smooth decay. The right panels of Fig. 4 show the time evolution of the viscous energy dissipation in the region of interest. Lower VED values are obtained using the single orifice configuration, and the highest values are obtained in the case of symmetric double orifice configuration. In clinical settings, higher VED values in the LV are associated with higher energy consumption and risks of heart failure. Therefore, from the dissipation of energy standpoint, an asymmetric configuration might be a better solution when ETER is required.

Time-frequency spectra. In Fig. 5, the time-frequency spectra of the u-component of the velocity signals at various selected points are displayed for the three different configurations and formation times tested. For the single orifice configuration, the probed location was selected close to the outlet and aligned with the valve leaflet, while for double orifice configurations, a location in the middle of the region of interest is selected corresponding to $x/D = 1.75$ and $y/D = 0$. The time-frequency spectra for the single orifice configuration display faint high-frequency signals from $t/T = 0.3$–0.5. This is more noticeable for the highest formation time ($L/D = 2.5$). For double orifice configurations, a mix of low and high frequencies can be observed. This is more perceptible in the case of the symmetric double orifice where the low frequencies appear to be dominant and last for a significant time period. This seems to be significantly attenuated in the case of the asymmetric double orifice probably due to the side deflection of the jet moving the flow away from the probed point. The symmetric double orifice configuration appears to be the most critical configuration with regard to velocity fluctuations and induced turbulence. Figure 6 focuses on this configuration and displays the time-frequency spectra at nine different locations for $L/D = 1.9$. Note that the scale is different from the one in Fig. 5. The signals within the jet cores are rather turbulent, being strongly comprised of high frequencies. The region between the cores, although exhibiting significant shear, does not experience strong turbulence but is, instead, dominated by lower frequencies.

In conclusion, this experimental study aimed to evaluate, from a fundamental point of view, the flow structures in the near-field wake of a model of a mitral valve before and after simulating edge-to-edge repair. The results show that edge-to-edge repair leads to an interesting flow characterized by twin pulsed jets that merge

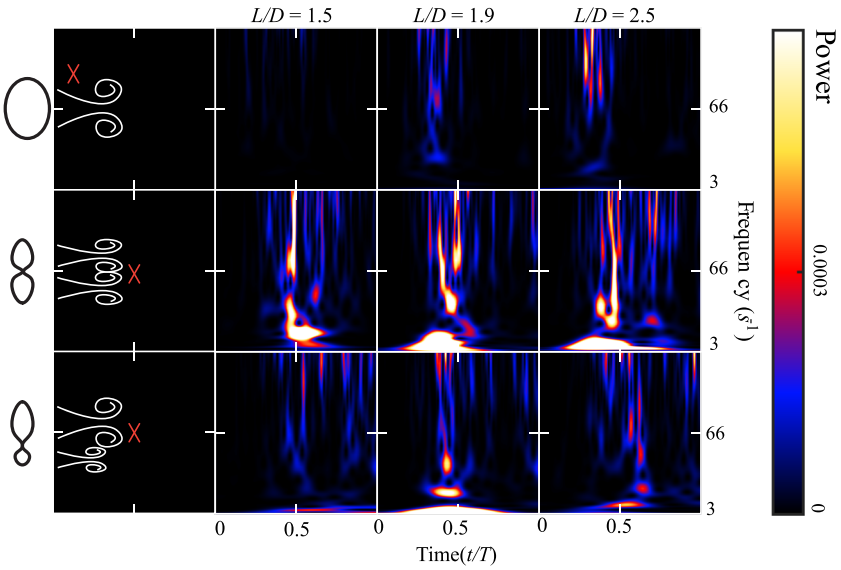

FIG. 5. Time-frequency spectra of the axial velocity component for all the orifice configurations and all L/D values. The red cross marks indicate the location in the region of interest where the velocity signals are extracted for time-frequency spectrum analysis.

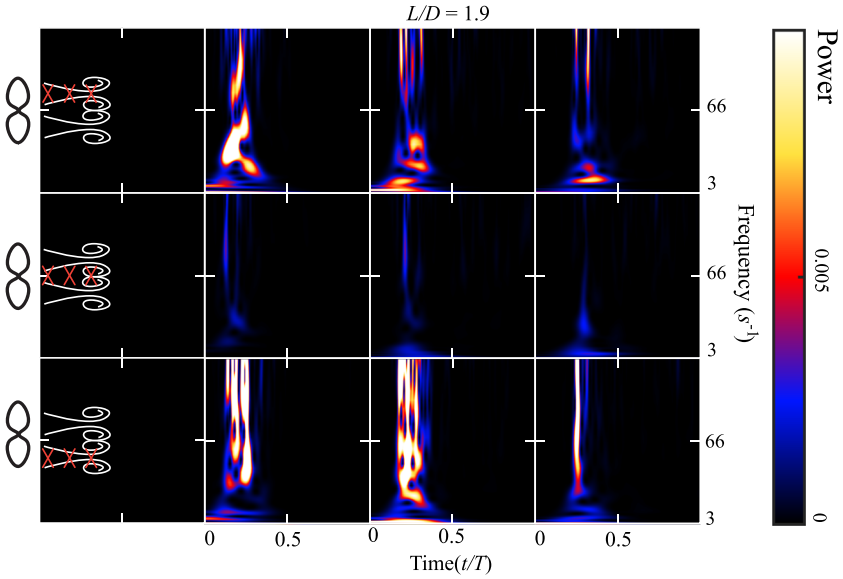

FIG. 6. Time-frequency spectra of the axial velocity component for the symmetric orifice configuration and *L*/*D* = 1.9. The red cross marks indicate the location in the region of interest where the velocity signals are extracted for time-frequency spectrum analysis.

farther downstream of the valve. This type of flow has not been extensively investigated in the literature, despite its current relevance not only to cardiovascular flows but also to underwater propulsion.[20,34] The investigation of the flow in terms of viscous energy dissipation and time-frequency spectra shows that the symmetric double orifice configuration leads to a sub-optimal performance compared to the single orifice and asymmetric orifice configuration. This result is important knowing that, in clinical practice, in the large majority of cases, the suture is positioned in the middle of commissures leading to a symmetric double orifice configuration. Obviously, *in vivo* studies are still required in order to confirm the impact of the above findings on left ventricle hemodynamics. Finally, future experimental studies are still required in order to evaluate the findings of this study under more physiologically realistic flow conditions that exist in a left ventricle and to evaluate, mostly in the cases with double orifices, the more complex three-dimensional flow structures that are certainly developing downstream of the orifice plane.

See the supplementary material for the videos of instantaneous velocity and vorticity fields, PIV technical details, and the validation for the single orifice configuration.

This work was supported by a grant from the Natural Sciences and Engineering Research Council of Canada (Grant No. 343164-07).

DATA AVAILABILITY

The data that support the findings of this study are openly available in github.com/msargordi/model_mitral_valve.

REFERENCES

[1]H. Baumgartner, V. Falk, J. J. Bax, M. De Bonis, C. Hamm, P. J. Holm, B. Iung, P. Lancellotti, E. Lansac, D. Rodriguez Munoz, and R. Rosenhek, "ESC/EACTS guidelines for the management of valvular heart disease," Eur. Heart J. **38**, 2739–2791 (2017).

[2]S. Pant and K. J. Grubb, "Percutaneous mitral valve technology: What is on the horizon?," in *Seminars in Thoracic and Cardiovascular Surgery* (Elsevier, 2017), Vol. 29, pp. 447–450.

[3]F. Grigioni, J.-F. Avierinos, L. H. Ling, C. G. Scott, K. R. Bailey, A. J. Tajik, R. L. Frye, and M. Enriquez-Sarano, "Atrial fibrillation complicating the course of degenerative mitral regurgitation: Determinants and long-term outcome," J. Am. Coll. Cardiol. **40**, 84–92 (2002).

[4]R. A. Nishimura, C. M. Otto, R. O. Bonow, B. A. Carabello, J. P. Erwin, L. A. Fleisher, H. Jneid, M. J. Mack, C. J. McLeod, P. T. O'Gara, V. H. Rigolin, T. M. Sundt III, and A. Thompson, "2017 AHA/ACC focused update of the 2014 AHA/ACC guideline for the management of patients with valvular heart disease: A report of the American college of cardiology/American heart association task force on clinical practice guidelines," J. Am. Coll. Cardiol. **70**, 252–289 (2017).

[5]S. Lazam, J.-L. Vanoverschelde, C. Tribouilloy, F. Grigioni, R. M. Suri, J.-F. Avierinos, C. De Meester, A. Barbieri, D. Rusinaru, A. Russo, and A. Pasquet, "Twenty-year outcome after mitral repair versus replacement for severe degenerative mitral regurgitation: Analysis of a large, prospective, multicenter, international registry," Circulation **135**, 410–422 (2017).

[6]O. Alfieri, F. Maisano, M. De Bonis, P. L. Stefano, L. Torracca, M. Oppizzi, and G. La Canna, "The double-orifice technique in mitral valve repair: A simple solution for complex problems," J. Thorac. Cardiovasc. Surg. **122**, 674–681 (2001).

[7]S. S. Goel, N. Bajaj, B. Aggarwal, S. Gupta, K. L. Poddar, M. Ige, H. Bdair, A. Anabtawi, S. Rahim, P. L. Whitlow *et al.*, "Prevalence and outcomes of unoperated patients with severe symptomatic mitral regurgitation and heart failure: Comprehensive analysis to determine the potential role of MitraClip for this unmet need," J. Am. Coll. Cardiol. **63**, 185–186 (2014).

[8]S. D. Kriechbaum, N. F. Boeder, L. Gaede, M. Arnold, U. Vigelius-Rauch, P. Roth, M. Sander, A. Böning, M. Bayer, A. Elsässer, and H. Möllmann, "Mitral valve leaflet repair with the new PASCAL system: Early real-world data from a German multicentre experience," Clin. Res. Cardiol. **109**, 549–559 (2020).

[9]F. Maisano, A. Redaelli, G. Pennati, R. Fumero, L. Torracca, and O. Alfieri, "The hemodynamic effects of double-orifice valve repair for mitral regurgitation: A 3D computational model," Eur. J. Cardiothorac. Surg. **15**, 419–425 (1999).

[10]Y. Hu, L. Shi, S. Parameswaran, S. Smirnov, and Z. He, "Left ventricular vortex under mitral valve edge-to-edge repair," Cardiovasc. Eng. Technol. **1**, 235–243 (2010).

[11]S. Lee and Y. A. Hassan, "Experimental study of flow structures near the merging point of two parallel plane jets using PIV and POD," Int. J. Heat Mass Transfer **116**, 871–888 (2018).

[12]R. N. Oskouie, M. F. Tachie, and B.-C. Wang, "Effect of nozzle spacing on turbulent interaction of low-aspect-ratio twin rectangular jets," Flow, Turbul. Combust. **103**, 323–344 (2019).
[13]T. Okamato, M. Yagita, A. Watanabe, and K. Kawamura, "Interaction of twin turbulent circular jet," Bull. JSME **28**, 617–622 (1985).
[14]T. Harima, S. Fujita, and H. Osaka, "Turbulent properties of twin circular free jets with various nozzle spacing," in *Engineering Turbulence Modelling and Experiments* (Elsevier, 2005), Vol. 6, pp. 501–510.
[15]A. Vouros and T. Panidis, "Influence of a secondary, parallel, low Reynolds number, round jet on a turbulent axisymmetric jet," Exp. Therm. Fluid Sci. **32**, 1455–1467 (2008).
[16]H. Li, N. K. Anand, Y. A. Hassan, and T. Nguyen, "Large eddy simulations of the turbulent flows of twin parallel jets," Int. J. Heat Mass Transfer **129**, 1263–1273 (2019).
[17]B. Zang and T. H. New, "Near-field dynamics of parallel twin jets in cross-flow," Phys. Fluids **29**, 035103 (2017).
[18]B. Zang and T. H. New, "On the wake-like vortical arrangement and behaviour associated with twin jets in close proximity," Exp. Therm. Fluid Sci. **69**, 127–140 (2015).
[19]K. Zhao, P. N. Okolo, Y. Wang, J. Kennedy, and G. J. Bennett, "An experimental characterization of the interaction between two tandem planar jets in a crossflow," J. Fluids Eng. **140**, 111106 (2018).
[20]A. G. Athanassiadis and D. P. Hart, "Effects of multijet coupling on propulsive performance in underwater pulsed jets," Phys. Rev. Fluids **1**, 034501 (2016).
[21]M. Jeyhani, S. Shahriari, and M. Labrosse, "Experimental investigation of left ventricular flow patterns after percutaneous edge-to-edge mitral valve repair," Artif. Organs **42**, 516–524 (2018).
[22]M. Gharib, E. Rambod, and K. Shariff, "A universal time scale for vortex ring formation," J. Fluid Mech. **360**, 121–140 (1998).
[23]M. Gharib, E. Rambod, A. Kheradvar, D. J. Sahn, and J. O. Dabiri, "Optimal vortex formation as an index of cardiac health," Proc. Natl. Acad. Sci. U. S. A. **103**, 6305–6308 (2006).
[24]M. Raffel, C. E. Willert, F. Scarano, C. J. Kähler, S. T. Wereley, and J. Kompenhans, *Particle Image Velocimetry: A Practical Guide* (Springer, 2018).
[25]L. Adrian, R. J. Adrian, and J. Westerweel, *Particle Image Velocimetry* (Cambridge University Press, 2011), Vol. 30.
[26]A. Sciacchitano, "Uncertainty quantification in particle image velocimetry," Meas. Sci. Technol. **30**, 092001 (2019).
[27]G. Batchelor, *An Introduction to Fluid Dynamics* (Cambridge University Press, Cambridge, UK, 1967).
[28]G. Pedrizzetti and F. Domenichini, "Nature optimizes the swirling flow in the human left ventricle," Phys. Rev. Lett. **95**, 108101 (2005).
[29]M. Stugaard, H. Koriyama, K. Katsuki, K. Masuda, T. Asanuma, Y. Takeda, Y. Sakata, K. Itatani, and S. Nakatani, "Energy loss in the left ventricle obtained by vector flow mapping as a new quantitative measure of severity of aortic regurgitation: A combined experimental and clinical study," Eur. Heart J. Cardiovasc. Imaging **16**, 723–730 (2015).
[30]G. Di Labbio and L. Kadem, "Reduced-order modeling of left ventricular flow subject to aortic valve regurgitation," Phys. Fluids **31**, 031901 (2019).
[31]A. Etebari and P. P. Vlachos, "Improvements on the accuracy of derivative estimation from DPIV velocity measurements," Exp. Fluids **39**, 1040–1050 (2005).
[32]N. E. Huang, Z. Shen, S. R. Long, M. C. Wu, H. H. Shih, Q. Zheng, N.-C. Yen, C. C. Tung, and H. H. Liu, "The empirical mode decomposition and the Hilbert spectrum for nonlinear and non-stationary time series analysis," Proc. R. Soc. London, Ser. A **454**, 903–995 (1998).
[33]J. O. Dabiri and M. Gharib, "The role of optimal vortex formation in biological fluid transport," Proc. R. Soc. B **272**, 1557–1560 (2005).
[34]K. R. Sutherland and D. Weihs, "Hydrodynamic advantages of swimming by salp chains," J. R. Soc., Interface **14**, 20170298 (2017).